*Jordan Journal of Civil Engineering,* Volume **15**, No. **1**, **2021**

# Seismic Behavior of Reinforced Concrete Rectangular Water Tank on Grade with Wall Opening

***Rasha F. Hassan [1], Hussam K. Risan [2] and Haitham A. Hussein [3]***

[1] M.Sc. Student, Department of Civil Engineering, Al-Nahrain University, Iraq.
E-Mail: rashaflayeh@gmail.com
[2] Assistant Professor, Department of Civil Engineering, Al-Nahrain University, Iraq.
E-Mail: dr.hussamrisan@gmail.com
[3] Assistant Professor, Department of Civil Engineering, Al-Nahrain University, Iraq.
E-Mail: haithamalshami@yahoo.com

## ABSTRACT

Water tanks represent an important critical structure type for the provision of water necessary for continuation of life and firefighting purposes. The objective of this paper is to study the response of reinforced concrete rectangular tank on grade in the presence of cleanout hole under the effect of an earthquake. This numerical analysis was conducted using nonlinear finite element three-dimensional models using ABAQUS. The water in the tank was modeled according to the hydrodynamic effects by including both the impulsive and the convective parts combined with hydrostatic pressure. The sloshing action was simulated based on a three-dimension added-mass approach. Additionally, eleven numerical models were investigated to determine the critical position of the cleanout opening relative to the base of the tank and as a function of earthquake direction and peak ground acceleration. The results of the analysis illustrate that the presence of the embedded hole generates more wall stresses and strains. The strain around the opening enhances by increasing the peak ground acceleration and through enlarging the opening. The results also prove that the critical position of the opening happens when the wall is parallel to the direction of the seismic force and when the opening is placed near the base of the tank.

**KEYWORDS:** Water tank, Impulsive and convective parts, Added-mass model, Wall opening.

## INTRODUCTION

Generally, a reinforced concrete water tank on grade is divided into two categories based on its wall-to-foundation connection. The first category is characterized by a non-sliding or fixed base, where the fixed or hinged wall-to-foundation connection is usually assumed. The second category is characterized by a flexible base. The flexible base permits movement or motion in different degrees or levels based on the wall-to-foundation boundary conditions. According to this concept, the latter category is further classified into either anchored or unanchored contained and unanchored uncontained. All the types of the second category are usually used in ground cylindrical tanks of large sizes to accommodate circumferential strain comfortably. The connection type has a large influence on the response of the concrete water tank on grade, especially in resisting seismic forces (ACI 350.3, 2006; Munshi, 2002).

Liquid reservoirs are considered as essential structures in case of an earthquake for their essential functions in providing water necessary for life and firefighting services. Unfortunately, the water tank shows always a poor performance under moderately severe ground motions due to the additional hydrodynamic pressure resulting mainly from the water sloshing effect. The weak performance in this type of structure may be related to the various inlet and outlet pipes. These holes convert the wall of the tank from a continuous medium into discontinuous region, where stresses are concentrated near these openings. Poor performance usually commences with minor cracks at

Received on 1/7/2020.
Accepted for Publication on 21/9/2020.

low applied stresses and ends with collapse at a large peak ground acceleration magnitude of the considered earthquake. There are many examples of liquid tanks that have collapsed when subjected to earthquakes' force. For instance, the famous two damages of storage tanks caused in 2011 and 2013 under Tohoku earthquake and Marlborough earthquake in New Zealand, respectively (Hatayama, 2015; Yazdanian et al., 2019), are a compelling evidence for this phenomenon. Other water tank disasters that occurred under Jabalpur earthquake in 1997 (Rai, 2002), Bhuj earthquake in 2001 (Rai, 2002) and Kaikōura ground motion (Yazdanian et al., 2019) have been recorded in the literature.

Numerous studies in the literature were carried out to investigate the response of reinforced concrete water reservoirs under different earthquake magnitudes. The overall purpose of these experiments is to keep the tank in operational condition after exposure to several seismic forces. Veletsos (1974) studied the performance of water tanks based on both rigid and flexible foundations under horizontal ground motion. The results of Veletsos proved that foundation flexibility does not affect the tank wall convective pressure distribution. Besides, the sloshing component of the hydrodynamic pressure is not affected by either the tank wall flexibility or the supporting soil medium. Later on, Haroun (1980) investigated the unstable response of versatile cylindrical liquid tanks based on a developed mechanical model which is identical to the well-known Housner model, but is applicable to versatile tanks. At the same time, Tedesco (1983) conjointly with Haroun studied the vibration characteristics and unstable response of cylindrical liquid storage tanks. The latter study confirmed that wall flexibility has a solely considerable impact on impulsive pressure, whereas convective pressure was not plagued by wall flexibility. Malhotra (1997) proposed the base-isolated problem of tank structure under a horizontal earthquake. Base isolation problem is defined as a connection-free case between the wall and the foundation base plate. The results demonstrated that base isolation significantly reduces both base shears and axial stresses in addition to overturning moment.

Chen and Kianoush (2009) developed a simple way for dynamic analysis of reinforced concrete rectangular water tanks. They simulated the tank as a single degree-of-freedom system (SDOF) with generalization approach. The consistent mass approach was used in this analysis. The effect of tank wall flexibility as related to hydrodynamic pressures was investigated. The results indicated that tank wall flexibility is considered an important parameter in the calculation of hydrodynamic pressures. The results also confirmed the combination of the generalized SDOF with the design response spectrum method in the vibration problem of such structure. Furthermore, Ghateh et al. (2015) analyzed two types of pedestal models with opening-supported elevated water tanks under earthquake. This analysis was carried out using finite element software (ANSYS). These models individually have two height-to-diameter ratios of 2.9 and 1.3 for opening dimensions 3 × 3m and 3.7×3.7 m. Every model was analyzed three times to represent the three earthquake directions with respect to the opening to catch the critical position of the hole. The seismic analysis results showed that direction 1 which is parallel to the opening is considered as the critical one. Amal Al-Far and Salam Al-Far (2016) studied a reinforcement concrete structure under Aqaba earthquake in 1995. The structure implemented a non-linear three-dimensional model using SAP2000 software and was subjected to Aqaba earthquake. The results of the numerical study (shear strength, bending moment, compressive and tensile stresses) were compared with the actual damage to this structure, where a great match was observed.

Kumar et al. (2016) analyzed three sizes of liquid-containing rectangular tanks subjected to an earthquake. Every size has five different height-to-length ratios. In this experiment, different codes, such as IS 1893 Part 2, ACI 350.3, IS 3370 Part IV-1967 and Eurocode, 8 were used. The study aimed to develop design charts that specify the share of impulse and convective weights from the total weight of water and their impact point in case of dynamic analysis. Also, the accuracy of two Indian codes was checked based on shear and moment in the wall base. The results substantiated that shear and moment at the base using IS 1893-Part 2 in the dynamic case were recommended higher than the values obtained by IS 3370 IV-1967 in the static one. This study also recommends that the IS 3370 IV-1967 code needs to be updated to be more accurate and reliable. Besides, the results indicated that the difference in the height-to-

length ratio with constant tank size has an effect on the values of shear and moment at the base. Hazirbaba et al. (2019) discussed the approaches used in designing earth-retaining structures under seismic forces. This study presented modern technology in designing these structures under earthquakes. The study showed that the actual loading of this structure is very complicated, especially when subjected to an earthquake; so, a false method was used to estimate the applied pressures. This method allows for permissible deformation and estimates the dimensions of the structure, especially in seismic regions with an acceleration greater than 0.29g. Deoda et al. (2020) studied two earth dams under the influence of different time history earthquakes. This structure was carried out using Studio 2012 software. The results showed that the water level in the reservoir has a great influence on dam deformation.

In summary, the previous trials have proved that wall flexibility of the tank is only responsible for a marginal change in impulsive pressure. Base isolation of the tank under a horizontal earthquake reduces the overturning moment, base shear and axial stresses. Height-to-length ratio of the tank affects the magnitude of hydrodynamic pressure. Not to mention that the maximum response of pedestal with openings that supported elevated water tanks' underground motion depends on the earthquake direction relative to the opening position. The general aim of this study is to perform a numerical seismic analysis of on-grade reinforced concrete water tank with an embedded cleanout hole in its walls. What is more, hydrodynamic effects from both impulsive pressure and convective pressure due to ground motion are investigated. With the help of the added-mass approach in three- dimensional modeling, the sloshing action of the convective part is adopted in this analysis. The code model available methods for calculating the response of on-grade water tank are studied and compared with our numerical model. In view of the aforementioned, a parametric study based on the earthquake direction to the opening position, opening size, earthquake type and peak ground acceleration values is conducted.

**Method and Modeling**

**Model Codes:** Usually, the water tank is modeled using Housner's method. This approach assumes approximately that the total hydrodynamic impact due to earthquake loading can be found as a summation of two components. The first component is named the impulsive one. The water part at the bottom of the tank manages the impulsive component. The second component is titled as convective (sloshing). The water part at the top of the tank is in control of the convective component. Fig.1 shows a rectangular tank of length "L" and width "B" with water height "$H_L$". The bottom water part is represented by ($W_I$) which is designated as the impulsive weight of liquid. This weight is modeled as a rigid mass added to the tank at height "$h_I$". The water part at the top of the tank is represented by ($W_C$) which is designated as the convective weight of the liquid. This weight is modeled as a rigid mass equivalent to the water convective portion attached to the tank wall by springs of appropriate stiffness and with an appropriate amount of damping. The point of action of the convective weight is at height "$h_C$".

According to the above model, the water tank can be treated dynamically as a two-degree-of- freedom system. These two degrees of freedom resulting from impulsive and convective components have separate periods. For this reason, the overall response of the tank under earthquake can be determined by the square root of the sum squares "SRSS" of the individual response due to both impulsive and convective parts. The base shear, overturning moment and wall pressure in the water tank due to ground motion can be calculated approximately by many codes, like International Building Code (IBC 2000), Uniform Building Code 1997 (UBC´97), Uniform Building Code 1994 (UBC´94), BOCA National Building Code 1996 (BOCA´96) and Standard Building Code 1997 (SBC´97), in addition to Seismic Design of Liquid-containing Concrete Structures and Commentary (ACI 350.3-6). IBC2000 equations are adopted in this study for verification purposes (Housner, 1963; Haroun and Housner, 1981).

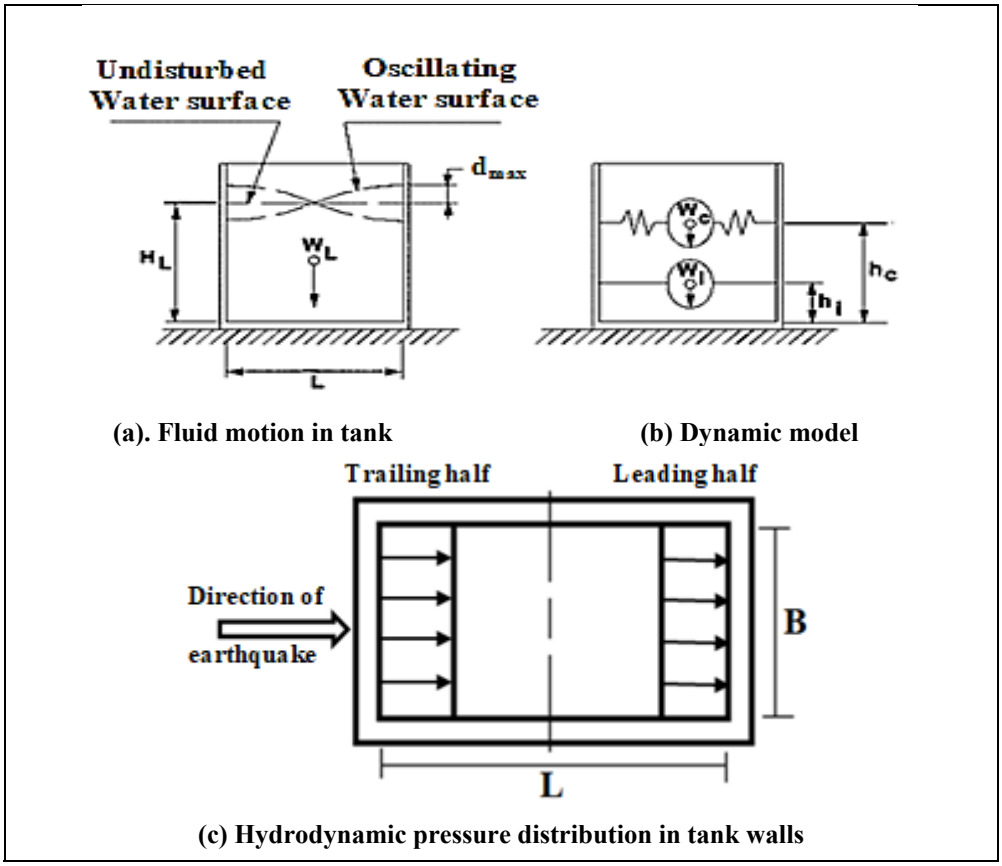


**Figure (1): Tank dynamics (ACI 350.3, 2006)**

The basic shear equation of the International Building Code (IBC 2000) is modified to include both the impulsive part and the convective part.

$$V_I = C_{SI}(W_w + W_R + W_I) \quad \text{Impulsive} \tag{1}$$

$$V_C = C_{SC}W_C \quad \text{Convective} \tag{2}$$

Then, the total base shear is calculated as:

$$V_T = \sqrt{V_I^2 + V_C^2} \tag{3}$$

where $V_I$, $V_c$ and $V_T$ are impulsive, convective and total shears, respectively. The quantities $W_w$, $W_R$, $W_I$ and $W_C$ are the overall weight of the tank walls, weight of roof-if any, water weight share due to the impulsive component and water weight share due to the convective component, respectively. The weight of impulsive $W_I$ with its centroid $h_I$ and the convective weight $W_C$ with its centroid $h_C$ can be determined for on-grade rectangular water tank as a portion of the overall water weight from Fig.2. The quantities $C_{SI}$ and $C_{SC}$ are determined based on the equation of the code chosen according to impulsive and convective periods that depend on the important factor, seismic coefficient, as well as the design acceleration spectral response at short period and 1-second period.

The overturning moment at the base of the tank for the hydrodynamic components can be written as follows:

$$M_I = C_{SI}(W_w h_w + W_R h_R + W_I h_I) \text{ Impulsive} \tag{4}$$

$$M_C = C_{SC}(W_C h_C) \text{ Convective} \tag{5}$$

where $h_w$ and $h_R$ are the heights of wall inertia and roof inertia, respectively. The total overturning moment can be calculated as:

$$M_T = \sqrt{M_I^2 + M_C^2} \tag{6}$$

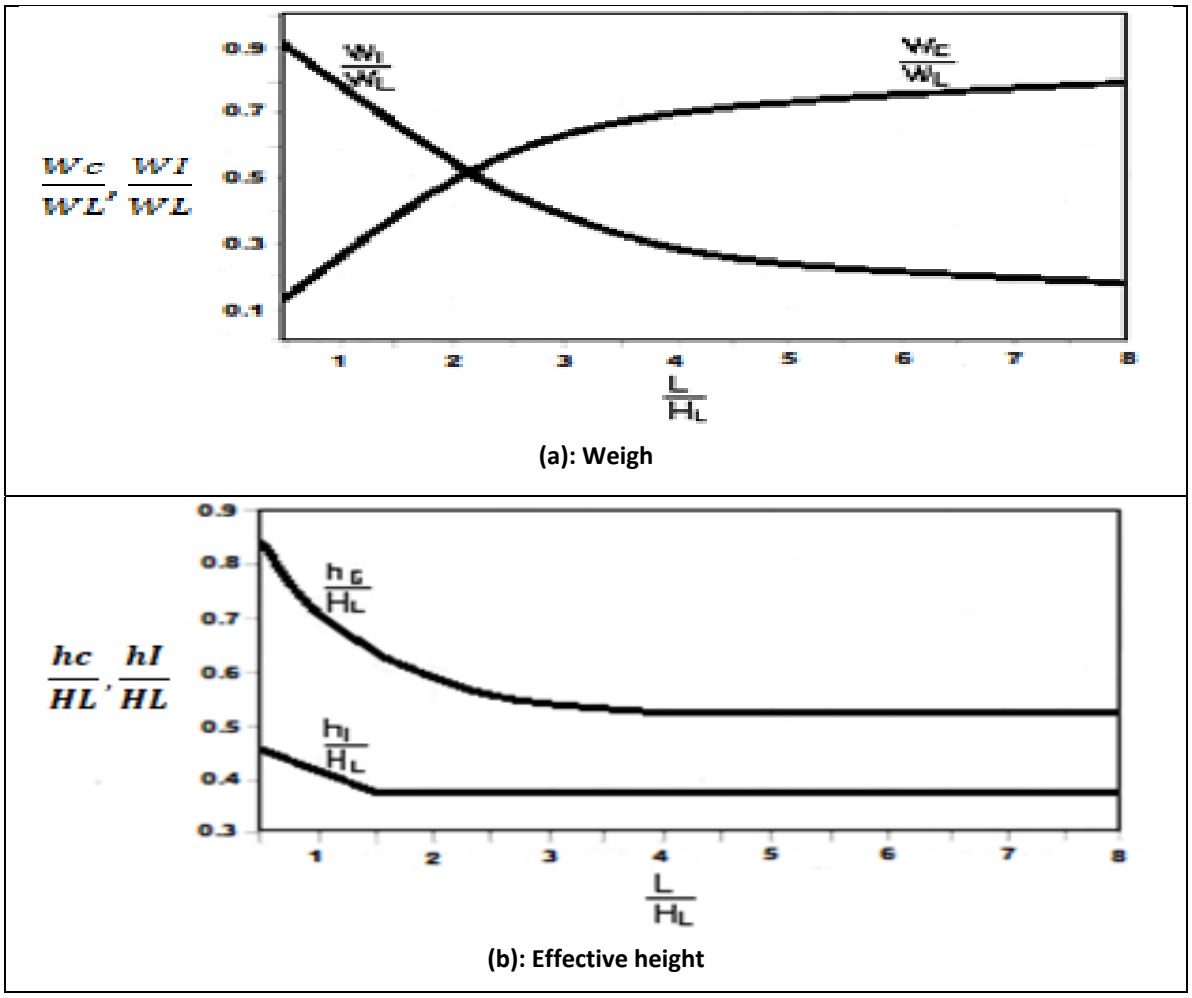


**Figure (2): Impulsive and convective weights and their effective heights (Haroun and Housner, 1981; Housner, 1963)**

The equations for determining the impulsive period $T_I$ and the convective period $T_C$ of rectangular water tanks are necessary to calculate the seismic coefficient required for both base shear and overturning moment. There are some guidelines to estimate $T_I$ boundary based on the foundation-to-wall connection and tank deformation (Munshi, 2002). The following suggested equation can be utilized to find the period due to impulsive component in a rectangular tank:

$$T_I = 2\pi\sqrt{\frac{W}{gK}} \quad (7)$$

"K" wall stiffness parameter can be calculated for a fixed-base constant-thickness cantilever wall as:

$$K = \frac{E_C}{4\times10^6}\left(\frac{t_w}{h}\right)^3 \quad (8)$$

where $W = W_W + W_R + W_I$ and "h" is the average height of the inertia force of the tank with its contents that were assumed to act. $t_w$ is the thickness of the tank wall, $E_c$ is the concrete modulus of elasticity and g is the gravitational acceleration. The periods associated with the convective component $T_C$ and the stiffness $K_C$ can be determined as:

$$T_C = \frac{2\pi}{\lambda}\sqrt{L} \quad (9)$$

$$k_c = \frac{4\pi^2 W_c}{T_c^2 g} \quad (10)$$

where L is the tank length in the direction of analysis and $\lambda$ is a function of L and $H_L$.

The concrete structure of the tank with its baffle walls, piping fixtures and joints should be designed to resist the highest stresses that result from different

applicable forces. This condition is required to fulfil the required overall water tank performance. The walls perpendicular to the direction of the analysis are considered as a danger element. The combined effects of both statics and dynamics are used to design such walls according to the applicable load combination illustrated in the adopted international code. In the International Building Code (IBC 2000), this combination, for example, is as follows:

$$U = 1.2D + 1.0E + 1.2F \quad (11)$$

where U is the total load, D is the dead load, E is the effect of earthquake and F is the effect of hydrostatic fluid pressure. For rectangular tanks, both impulsive and convective forces on the walls can be calculated as:

$P_W = C_{SI} W_W$ Wall inertia (based on two walls perpendicular to the direction of motion) (12)

$P_I = C_{SI} W_I$ Impulsive force (13)

$P_C = C_{SC} W_C$ Convective force (14)

Thus, the forces at any height "y" on the wall due to inertial effect, impulsive and convective components are written as follows:

$P_{Wy} = \frac{P_W}{2H_W}$ (remember that $P_W$ is based on the weight of two walls) (15)

$P_{IY} = P_I \frac{(4H_L - 6h_I) - (6H_L - 12h_I) \times \frac{y}{H_L}}{2H_L^2}$ Impulsive (16)

$P_{CY} = P_C \frac{(4H_L - 6h_C) - (6H_L - 12h_C) \times \frac{y}{H_L}}{2H_L^2}$ Convective (17)

The two walls of the tank (B), perpendicular to the direction of the seismic forces, are divided into two parts, the first of which is the leading part and the second one is the trailing part, as shown in Fig.1c. Each wall is designed to resist a half of the impulsive, convective and inertia forces (Munshi, 2002). In this method, the moment in x and y directions, bottom and side shear and deflection on the wall are calculated based on the coefficient method, which is based on the theory of plate analysis (Munshi, 1998). This method is an approximate method for finding moment and shear, especially when there are many holes in the walls. The holes are implemented for inlet and outlet piping purposes.

**Water-Structure Interaction**

The analysis of on-grade water tank under earthquake as a liquid-structure interaction problem may be solved by utilizing several methods, such as the approximate method mentioned above in the model codes. In this method, the first approximation is due to the simulation of the sloshing effect on the tank, which is based on previously prepared charts. The second approximation, on the other hand, is in finding the moment and shear in the wall of the tank based on plate analysis theory according to the so-called coefficient method. In this approximate method, the hole due to inlet and outlet piping is neglected. There is another method that is considered much more accurate in these cases, which is named as the added-mass approach. The analysis in the added-mass approach can be conducted through the finite element method. The added-mass concept as displayed in Fig.1b can be analyzed by using some of the conventional FEM software, such as ABAQUS. In this approach, the convective weight $W_C$ and its location are calculated according to charts (Fig.2) and modeled as a rigid mass, respectively. The rigid mass is connected with the walls of the tank by appropriate springs. The impulsive weight $W_I$ is added to the wall of the tank as additional weight. After the tank is subjected to actual ground motion, the isolated mass exerts dynamic convective pressure on the tank walls according to their stiffness. The moment and shear calculated on the walls may be represented as the real stiffness contribution due to impulsive and convective pressures. Also, in this approach, the discontinuity regions in the walls of the tank, due to the holes, result from inlet and outlet piping, taking their effect on the maximum stress and strain in the walls into consideration.

**Finite Element Analysis**

Concrete rectangular on-grade tank free at the top with a rigid base was analyzed in this study. The properties and geometry of the tank are illustrated in Table 1, Fig.3 and Table 2. Imperial Valley 19$^{th}$ May 1940 and Hollister City Hall, 11/28/1974 earthquakes are applied to the water tank as typical input ground motions. The two earthquake profiles are shown in Fig.4. The Imperial Valley peak ground acceleration is

0.281g with a total time of 53.69 seconds. The Hollister City Hall peak ground acceleration is 0.089g with a total time of 33 seconds.

**Table 1. Properties of the rectangular tank (Munshi, 2002)**

| Parameter | Value |
|---|---|
| Specific weight of contained liquid ($\gamma_L$) | 10 kN/m$^3$ |
| Concrete strength ($f_{\acute{c}}$) | 28 MPa |
| Specific weight of concrete ($\gamma_C$) | 24 kN/m$^3$ |
| Modulus elasticity of concrete ($E_C$) | 26000 MPa |
| Steel strength ($f_y$) | 414 MPa |
| Wall thickness | 460 mm |
| Base thickness | 610 mm |
| $S_1 = 0.5$ , $S_S = 1.275$, $F_a = 1$, $F_v = 1.5$, Seismic coefficient R=2, Importance Factor =1 | |

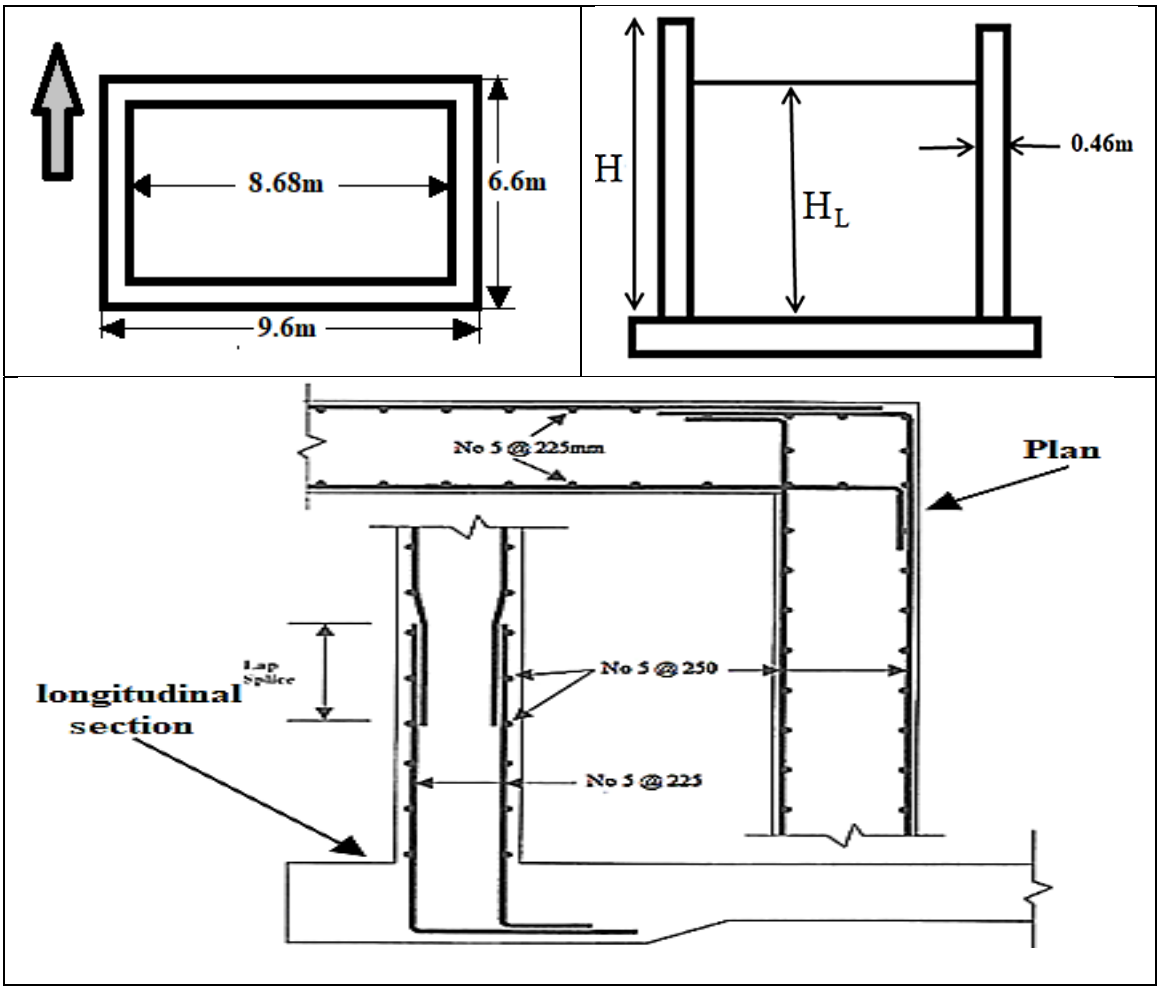


**Figure (3): Details of the tank (Munshi, 2002)**

In this study, elven numerical models of water tanks were run by ABAQUS based on the added-mass approach in three-dimensional nonlinear simulations, as depicted in Fig. 5, where two groups of tanks of two different sizes were studied. The first group is composed of four tanks with a total depth of 3 meters, while the second group is of seven tanks with a total depth of 6 meters. Each group contains a tank without holes and other tanks with

different hole diameters, different hole positions and different earthquake directions, as illustrated in Table 2. In this paper, the concrete and reinforcement rebars are modelled by C3D8R element and T3D2 element, respectively. Concrete properties, such as modulus of elasticity and the Poisson's ratio of 0.15, are used as input data for the elastic stage of the analysis. Damage plasticity model is used to simulate the concrete behaviour in the plastic stage. As for the parameters of the damage plasticity model, the dilation angle is taken equal to 31, eccentricity is taken as 0.1, $f_{b0}/f_{c0}$ is the ratio of initial equibiaxial compressive yield stress to initial uniaxial compressive yield stress. The default value of this ratio is taken as 1.16, K is the ratio of the second stress invariant on the tensile meridian to that on the compressive meridian, at initial yield for any given value of the pressure invariant. The default value for K is taken as 2/3 and the viscosity parameter is taken as zero.

The concrete stress-strain curve in compression and tension is shown in Fig. 6 and Fig. 7. The properties of steel, such as modulus of elasticity, Poisson's ratio, tensile strength and stress-strain relationship, are used as input data for the model. The interaction between the concrete and reinforcement bars is carried out by using embedded construction in the wall and foundation and tie construction in the wall base connection. The element size length in the X-, Y- and Z -axes (mesh) is taken as 100 mm for all the walls of the water tank. The boundary conditions of the tank with movement in the Y-axis are $(U_1, U_3, UR_1, UR_2,\ UR_3 = zero$ and $U_2 = X_g)$, while the boundary conditions of tanks with movement in the X-axis are $(U_2, U_3, UR_1 UR_2,\ UR_3 = zero$ and $U_1 = X_g)$. Hydrostatic pressure $(\gamma \times h_L)$ is applied internally on the walls of the water tank. Finally, the convective mass is used as an added rigid mass and is modeled by C3D8R element. The volume of the convective mass was assumed to be equal to one cubic meter. The density of the convective mass was calculated as $(\rho_c = W_c/Volume)$. The convective mass is attached with walls at $h_c$ by appropriate equivalent springs with stiffness equal to $k_c$ according to Equation 10. The impulsive weight was calculated, converted into equivalent concrete weight and added to the walls (ABAQUS Manual, 2014).

**Validation of Finite Element Model**

In this section, the accuracy of the finite element analysis for water tank added-mass model, including element selection, material properties, boundary conditions, loadings, interaction, size of the elements (mesh) and both impulsive and convective effects, is verified. The verification is performed between the finite element analyses of the control model of the tank with solid walls designated (S-I) as compared with the approximate analysis based on model codes. The geometry and properties of (S-I) solid tank are illustrated in Table 1, Table 2 and Fig.3. The validation analysis is performed based on elastic stage behaviour to match the behaviour that was assumed in the model codes used for this verification. In the model code analysis, hydrodynamic pressures were calculated based on IBC2000 code. A true earthquake (Imperial Valley) was chosen, which was equivalent to the values of the seismic coefficients of short period and one-second period used in the code method (Table 1). It can be elucidated that the displacement diagram in the middle of the free end of the long walls using ABAQUS was identical to the displacement diagram obtained from the web site (Seismosoft, 2002), as shown in Fig. 8.

**Table 2. Geometry of numerical models**

| Depth of tank | Name | The diameter of the openings (m) | The direction of the seismic force | Height from tank base to centre of openings (m) |
|---|---|---|---|---|
| 3m | S-I | Solid wall | The Y-axis | NA |
| | S-II | 0.65 | The Y-axis (parallel to the opening) | 0.825 |
| | S-III | 0.65 | The X-axis (perpendicular to the opening) | 0.825 |
| | S-IV | 0.65 | The Y-axis (parallel to the opening) | 1.725 |
| 6m | T-I | Solid wall | The Y-axis | NA |
| | T-II | 0.65 | The Y-axis (parallel to the opening) | 0.825 |
| | T-III | 0.65 | The X-axis (perpendicular to the opening) | 0.825 |
| | T-IV | 0.65 | The Y-axis (parallel to the opening) | 1.725 |
| | T-V | 0.65 | The Y-axis (parallel to the opening) | 3.325 |
| | T-VI | 1.00 | The Y-axis (parallel to the opening) | 1.000 |
| | T-VII | 1.50 | The Y-axis (parallel to the opening) | 1.250 |

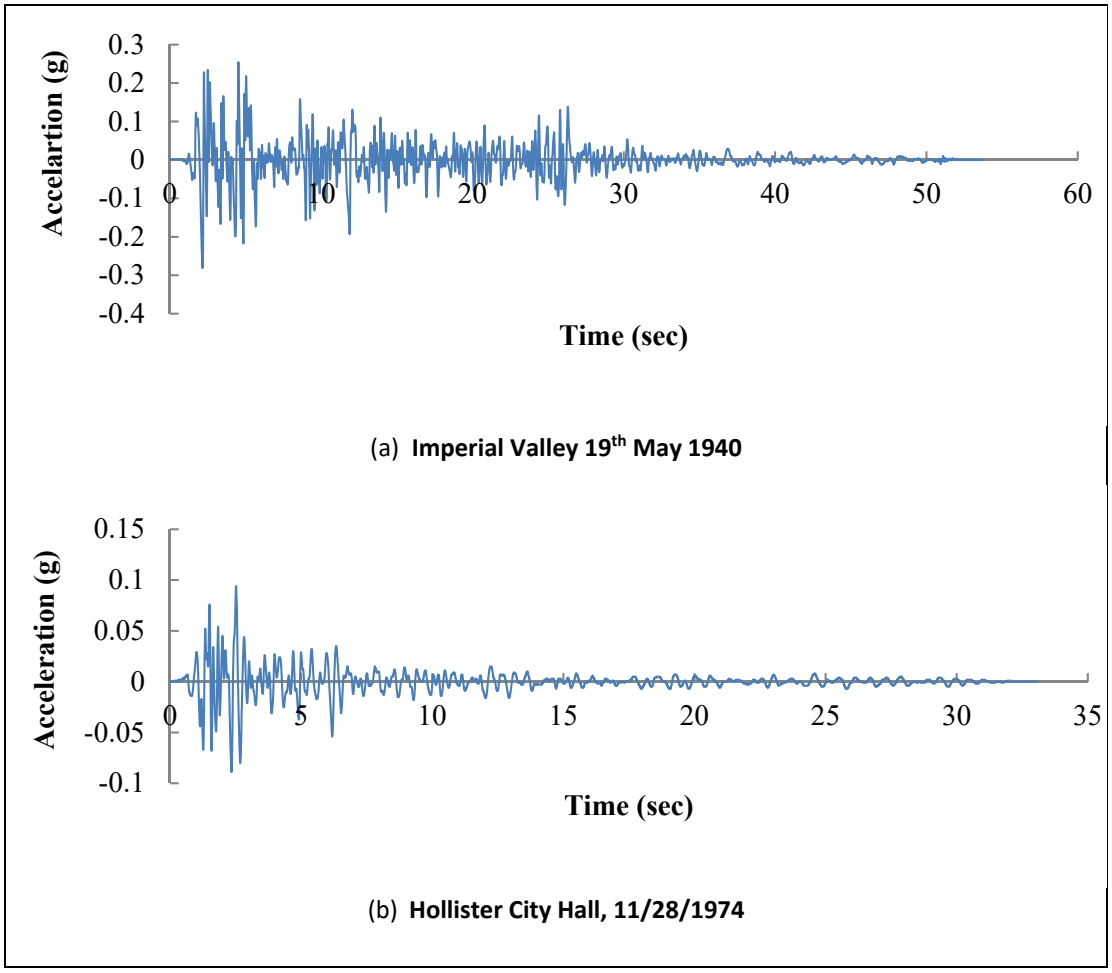


**Figure (4): Two input earthquake profiles (Seismosoft, 2002)**

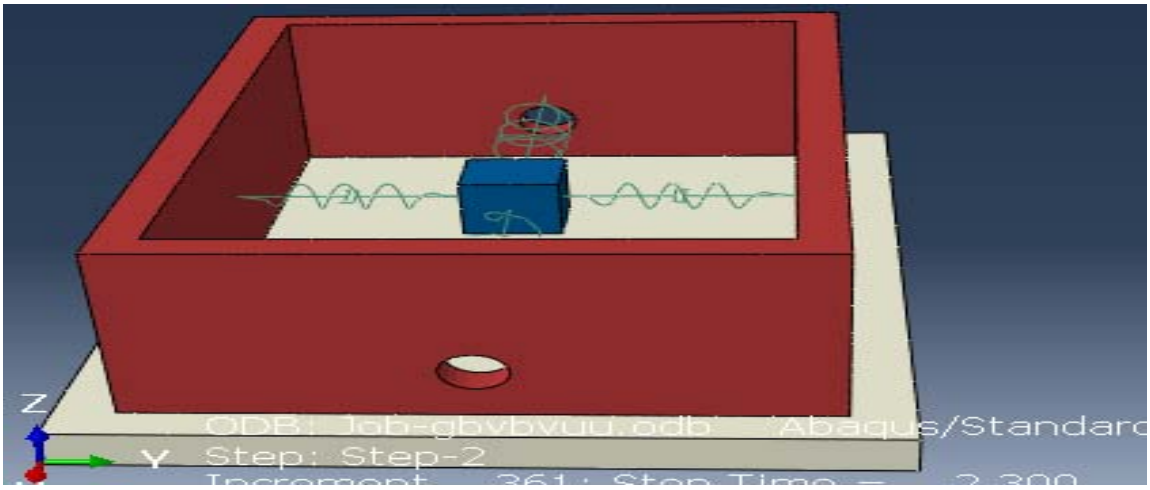


**Figure (5): Numerical runs in ABAQUS**

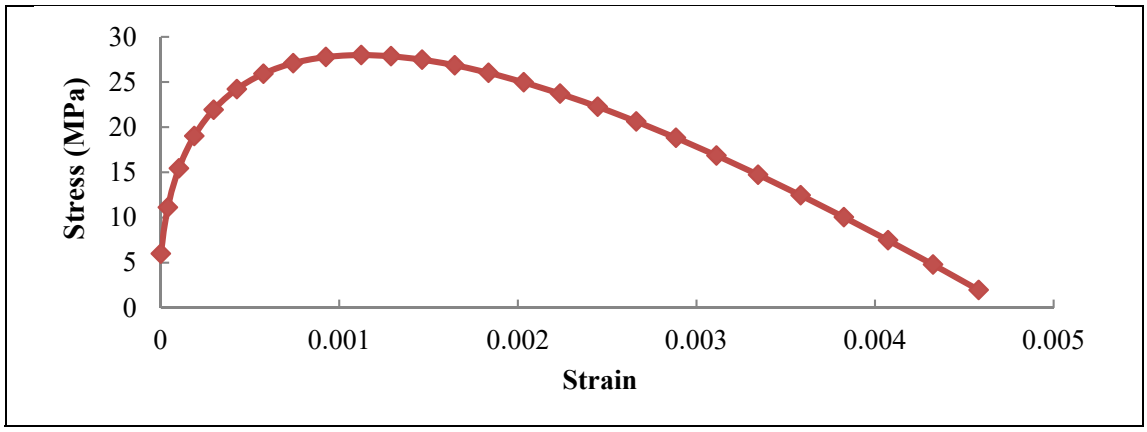


**Figure (6): Compression strength of concrete**

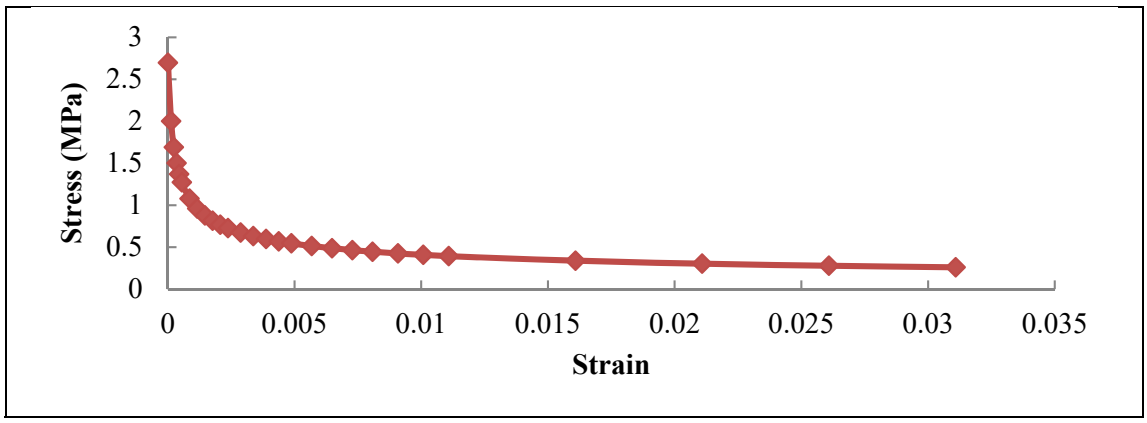


**Figure (7): Tension strength of concrete**

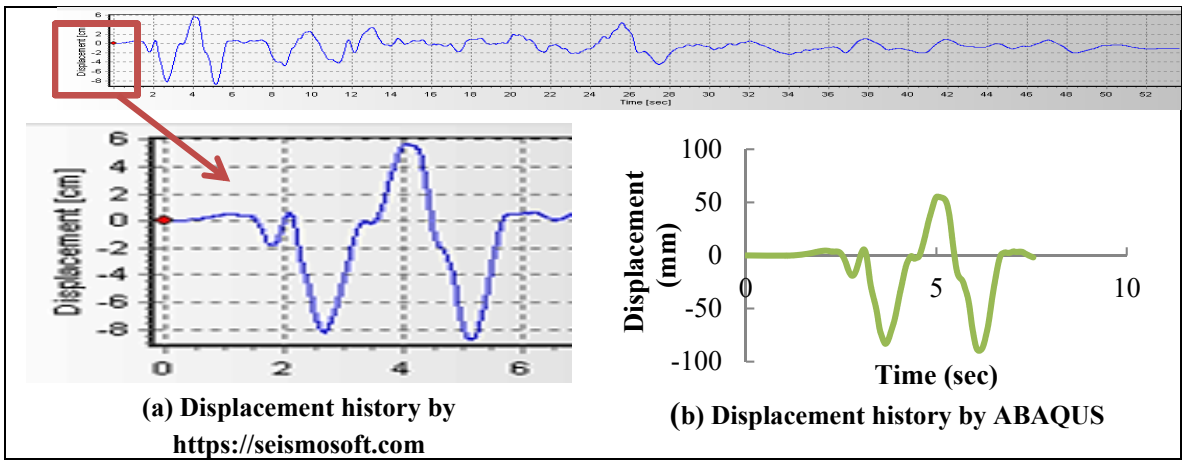


**(a) Displacement history by https://seismosoft.com**

**(b) Displacement history by ABAQUS**

**Figure (8): Displacement history at the middle free point of the longest wall**

The results of the comparison between model code and finite analysis in terms of maximum moment at the base of the tank wall perpendicular to the earthquake direction due to hydrostatic, inertia, impulsive and convective pressures are recorded in Table 3. Regarding these results, it can be claimed that the numerical model is in good match with the coded model in terms of maximum moment. In line with the above, the

ABAQUS model can be used for other run model tanks with openings. Fig.9 displays the time history of the moment at the base of the wall perpendicular to the earthquake direction. This figure illustrates that the maximum moment has occurred at the same time as the maximum acceleration took place which is equal to 2.16 sec. This confirms that the finite element model analysis is correct.

**Linear *versus* Non-linear Behavior**

In this section, the linear elastic behaviour was compared with the nonlinear elastic-plastic behaviour in the tank model (S-I) under seismic effect. The material nonlinearity resulting from the behaviour of concrete and steel rebar was investigated. The elastic-plastic stage of concrete adopted in ABAQUS was based on the damaged plasticity properties of the model under pressure. The inertia pressure was increased for both models until the tank reached the plastic stage. Fig.10a shows the applied pressure on the inner surface at both long walls of the tank. The results of this study revealed that the maximum moment at the wall in the plastic analysis is 1097 kN.m, while the maximum elastic moment is 572 kN.m. Fig.10b illustrates the load of the wall *versus* deflection for both elastic and plastic models. The deflection was measured at the middle of the wall at the free end, as shown in Fig.10a. The deflection in plastic behaviour is greater than the elastic deflection. It is concluded that the water tank in plastic analysis withstands more displacement and maximum moment of the wall before complete collapse.

**Table 3. Comparison results between code model and finite element model**

| | $Max.M_{x(\text{vertical direction})} kN.m$ | | | |
|---|---|---|---|---|
| | **Hydrostatic** | **Inertia** | $SRSS = \sqrt{Impulsive^2 + Convective^2}$ | **Total** |
| Code Model Analysis | 23.3 | 19.5 | 13.5 | 56.3 |
| Finite Element Analysis | 23.8 | 21.7 | 14.5 | 60 |

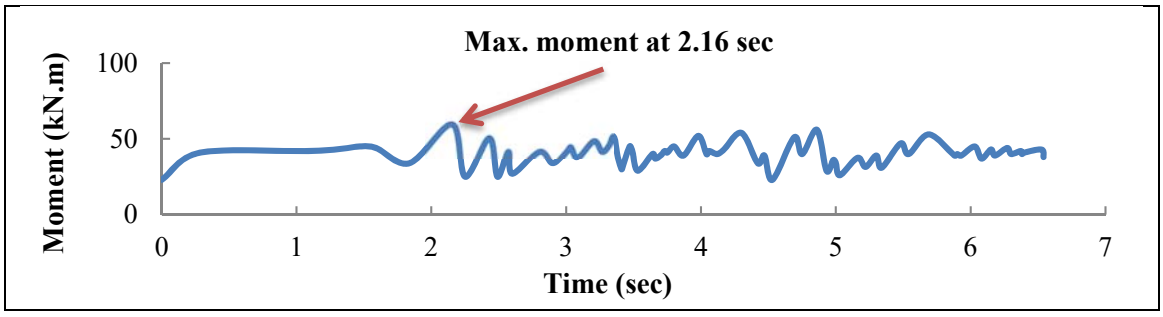


**Figure (9): Moment and acceleration histories at base of wall tank length**

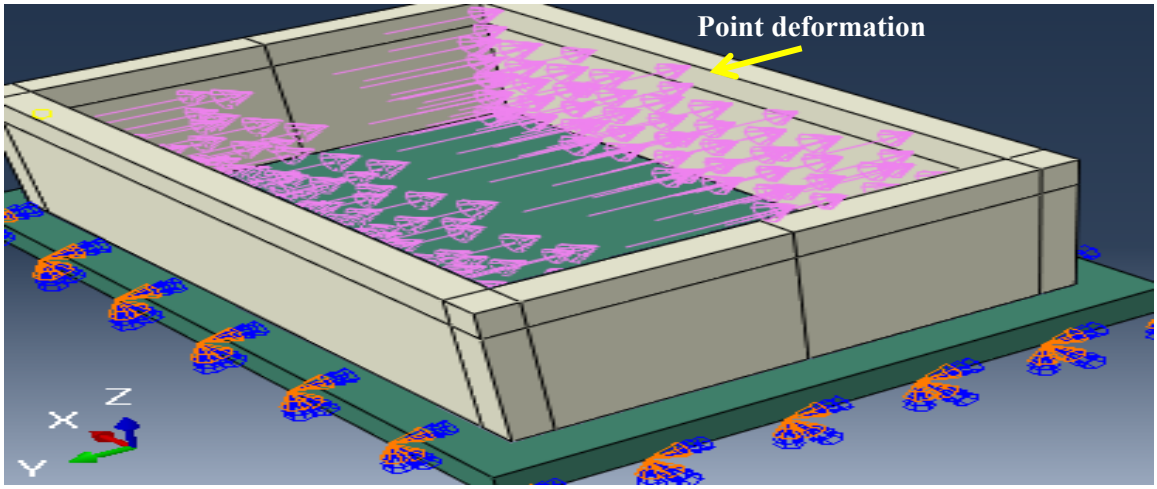


**(a). Model**

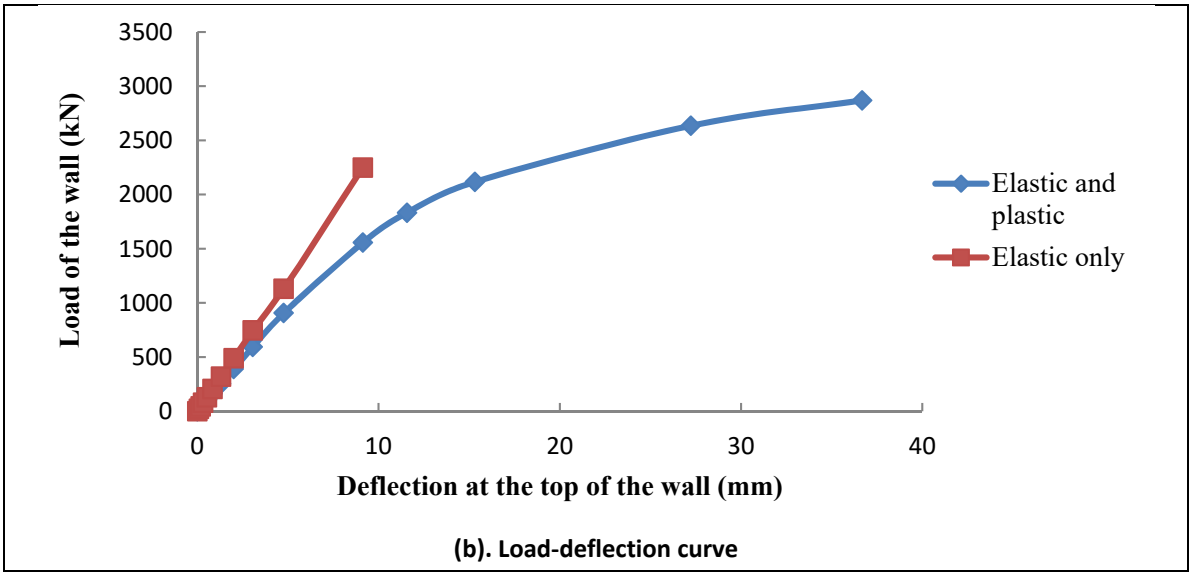


**Figure (10): Elastic and plastic behaviours**

**The Direction of Seismic Force Relative to the Opening**

In this section, the results of the models S-II and T-II, where the earthquake direction is aligned with the y-axis (parallel to the opening), are compared with those of the models S-III and T-III, where the earthquake direction is aligned with the x-axis (perpendicular to the opening). These tanks have a common opening diameter of 0.65m and an opening position of 0.825m from the base, as shown in Table 2. All the tanks are subjected to two base earthquakes (Imperial Valley and Hollister City Hall) illustrated in Fig.4 in addition to inflated Imperial Valley with a scale equivalent to three. The purpose of this section is to investigate the effect of the seismic force direction concerning the position of the hole either in the walls that are parallel or perpendicular to the loading direction. A path has been defined in ABAQUS to include the elements and the associated nodes surrounding the openings, as presented in Fig.11. The maximum principal stresses and strains are recorded for this path in Table 4 for all cases.

In cases 1 and 2 (elastic analysis), this table portrays that the maximum principal stresses and strains for all models under earthquake direction that are parallel to their openings are greater than their equivalent values at tanks the openings of which are perpendicular to ground motion direction. In the third case (Case 3, plastic analysis), the maximum principal stress in model S-II is less than the equivalent stress in model S-III, while the maximum principal plastic strain behaves differently, knowing that the elastic strains in both models are identical. This happened due to the non-linear behaviour of the tank, which was not noticed in the two models T-II and T-III, because they failed early.

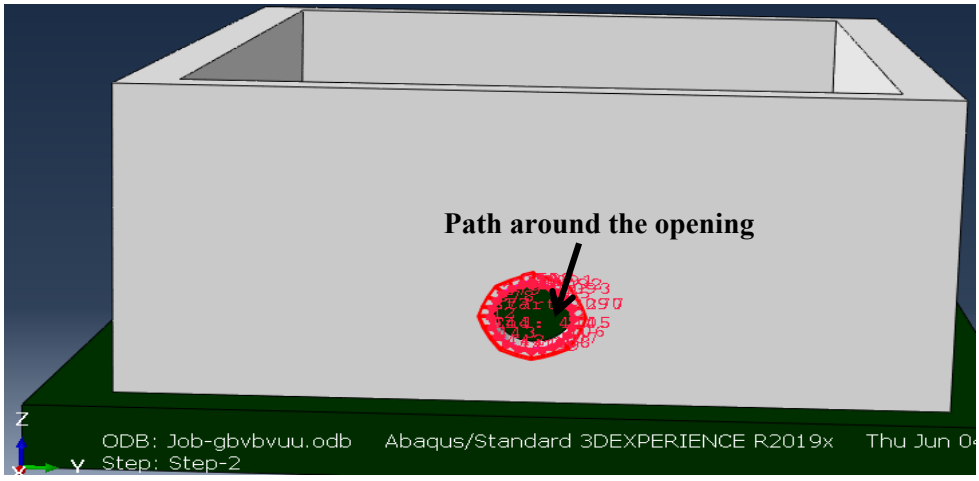


**Figure (11): The path around the opening**

**Table 4. Maximum principal stress and strain around the opening**

| Earthquake | | S-II Model | | | S-III Model | | |
|---|---|---|---|---|---|---|---|
| | | Stress (MPa) | Elastic Strain $\times 10^{-5}$ | Plastic Strain $\times 10^{-5}$ | Stress (MPa) | Elastic Strain $\times 10^{-5}$ | Plastic Strain $\times 10^{-5}$ |
| Case 1 | Imperial Valley | 5.20 | 7.23 | 0.00 | 4.17 | 3.21 | 0.00 |
| Case 2 | Hollister City Hall | 3.45 | 3.50 | 0.00 | 3.40 | 2.48 | 0.00 |
| Case 3 | Imperial Valley with scale 3 | 4.00 | 13.00 | 6.50 | 6.00 | 13.00 | 2.80 |
| Earthquake | | T-II Model | | | T-III Model | | |
| | | Stress (MPa) | Elastic Strain $\times 10^{-5}$ | Plastic Strain $\times 10^{-5}$ | Stress (MPa) | Elastic Strain $\times 10^{-5}$ | Plastic Strain $\times 10^{-5}$ |
| Case 1 | Imperial Valley | 2.50 | 3.00 | 0.00 | 2.36 | 2.00 | 0.00 |
| Case 2 | Hollister City Hall | 1.40 | 2.62 | 0.00 | 1.30 | 1.90 | 0.00 |
| Case 3 | Imperial Valley with scale 3 | 5.30 | 8.00 | 4.00 | 5.20 | 8.00 | 4.00 |

**Critical Height of the Opening Position**

In this section, the results of the models S-II and T-II, where the opening is placed at 0.825m from the base, are compared with those of the models S-IV and T-IV, where the opening is placed at 1.725m. Further, the results of model T-IV of 1.725m opening position from the base are compared to T-V of 3.325m opening position. These tanks have a common opening diameter of 0.65m and parallel earthquake direction to the direction of opening (critical direction), as indicated in Table 2. All the tanks are subjected to two base earthquakes (Imperial Valley and Hollister City Hall), as illustrated in Fig.4. The purpose of this section is to investigate the critical position of the opening. The same path depicted in Fig.11 has been defined in ABAQUS to perform this analysis. The maximum principal stresses in MPa and maximum nodal forces in Newton ($N_x$, $N_y$ and $N_z$) in x-, y- and z-axes are recorded for this path (Table 5) for all cases. Table 5 shows that the maximum principal stresses and the largest nodal resultant forces around the opening for the two models S-II and T-II are higher than their equivalent values for the two models S-IV and T-IV. Also, the maximum principal stress and the largest nodal resultant forces around the opening for model T-IV are higher than their equivalent values for model T-V.

**Table 5. Von-Mises node stresses and forces**

| Earthquake | S-II model | | | | S-IV model | | | | T-II model | |
|---|---|---|---|---|---|---|---|---|---|---|
| | Stress | $N_x$ | $N_y$ | $N_z$ | Sterss | $N_x$ | $N_y$ | $N_z$ | Stress | $N_x$ |
| Imperial Valley | 5.2 | 45 | 80 | 100 | 3.85 | 25 | 6.5 | 50 | 1.5 | 480 |
| Hollister City Hall | 3.45 | 100 | 300 | 750 | 1.97 | 90 | 150 | 550 | 1.4 | 480 |
| **Earthquake** | **T-II model** | | **T-IV model** | | | | **T-V model** | | | |
| | $N_y$ | $N_z$ | Stress | $N_x$ | $N_y$ | $N_z$ | Stress | $N_x$ | $N_y$ | $N_z$ |
| Imperial Valley | 60 | 130 | 1.36 | 360 | -200 | 110 | 0.8 | 360 | 35 | **88** |
| Hollister City Hall | 70 | 120 | 1.3 | 360 | 150 | 100 | 0.7 | 365 | 20 | **75** |

**Influence of Opening on the Wall Base Stresses**

In this section, the solid model S-I is compared with the model S-II, where the model S-II has a hole with a diameter of 0.65m located at a height of 0.825m from the base of the tank. The models S-I and S-II exposed to two base earthquakes (Imperial Valley and Hollister City Hall) are illustrated in Fig.4. Furthermore, the solid model T-I is compared with the models T-II, T-VI and

T-VII that have openings with a diameter of 0.65m, 1m and 1.5m located at an elevation from the base of 0.825m, 1.00m and 1.25m, one by one. These models are laid open to only one base earthquake (Imperial Valley) illustrated in Fig.4a. All models selected in this section are under parallel earthquake direction to the direction of the opening (critical direction), as illustrated in Table 2. The purpose of this section is to investigate the effect of the opening on the wall compared to the solid tank in terms of stress and strain. A path drawn by ABAQUS has been defined for all models above the opening (the top path), as shown in Fig.12.

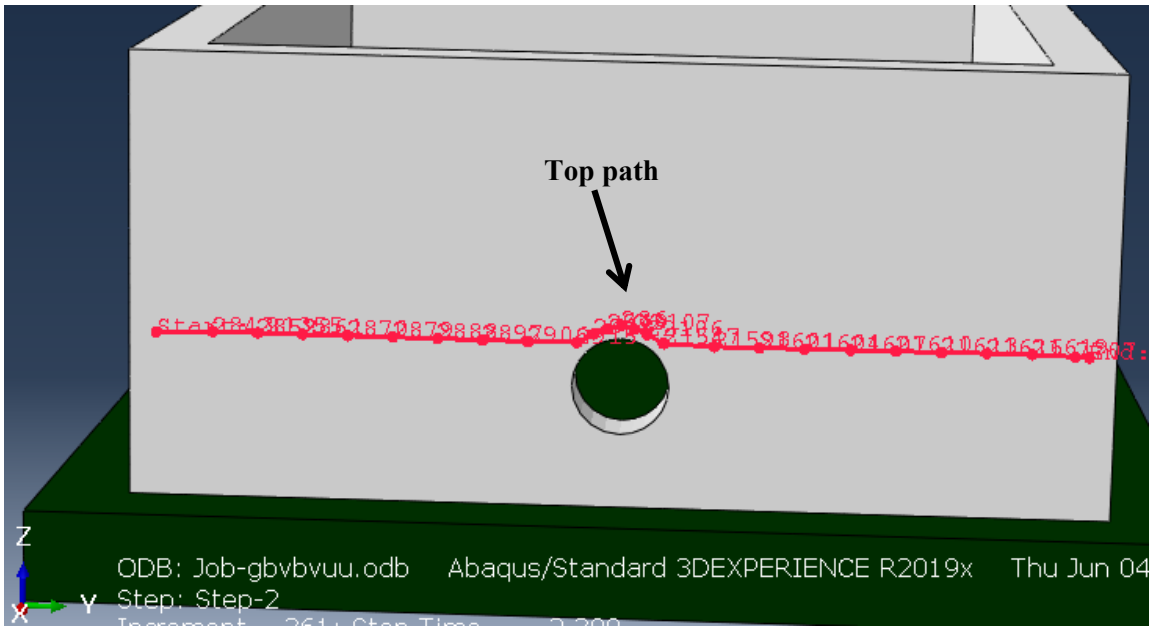


**Figure (12): The top path of the numerical model**

The results of the analysis uncovered that the stress distribution in the solid short wall is approximately equal to constant counter lines for each height, as shown in Fig.13a, while in Fig.13b, it appears that the stress of the short wall with the opening is concentrated in the sides of the openings. Von-Mises stresses and maximum principal strains of the top path of S-I and S-II for Imperial Valley and Hollister City Hall earthquakes are displayed in Fig. 14 and Fig. 15. Also, Von-Mises stresses of the top path of T-I, T-II, T-VI and T-VII for Imperial Valley earthquake are displayed in Fig 16.

As a matter of fact, Fig.14 unfolds that the Von-Misses stress at the top of opening for model S-II is 2.5MPa; whereas the stress in the equivalent place for model S-I is 1. 7MPa for case 1((Imperial Valley). In case 2 (Hollister City Hall), the stress at the top of opening for model S-II is equal to 1.0MPa; nevertheless, the equivalent value in model S-I is equal to 0.8MPa. Fig.15 shows that the strain at the top of opening for model S-II is $49\times 10^{-6}$, while the strain in the equivalent place for model S-I is $30\times 10^{-6}$for case 1. In case 2, the strain at the top of opening for model S-II is equal to $11\times 10^{-6}$, while the equivalent value in model S-I is equal to $6\times 10^{-6}$. Moreover, the results of the study lay out that the stress and strain at the top of an opening raise with increasing the diameter of the opening, as shown in Fig.16.

Von-Misses stress and maximum principal strain on the opening adjacent side node for model S-II in static and dynamic analyses are presented in Fig.17. The adjacent side node of the opening is manifested in Fig.13b. From Fig.17, it is observed that the value of stress and strain before the seismic force is applied to the tank (S-II) (static analysis) is 0.2MPa and $3.0\times 10^{-6}$, respectively. However, these values become 4.2MPa and $33.0\times 10^{-6}$, respectively, after seismic force (Imperial Valley earthquake) application to the tank (S-II) (dynamic analysis).

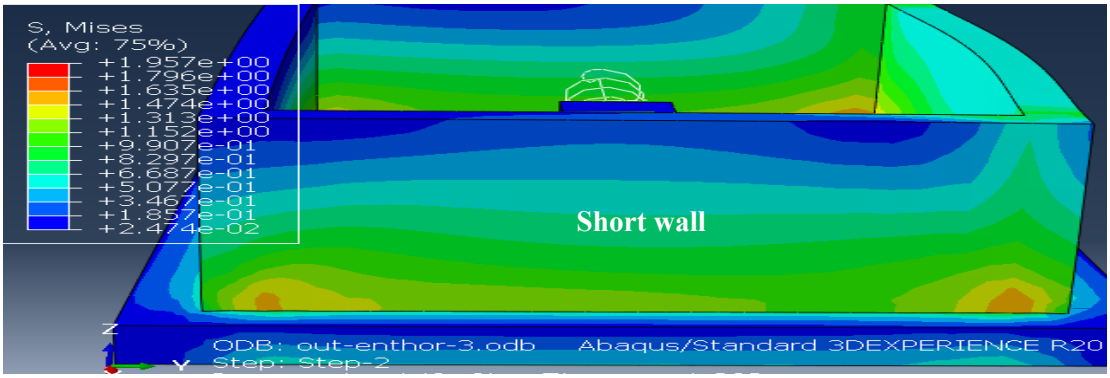


**(a) Solid-wall tank**

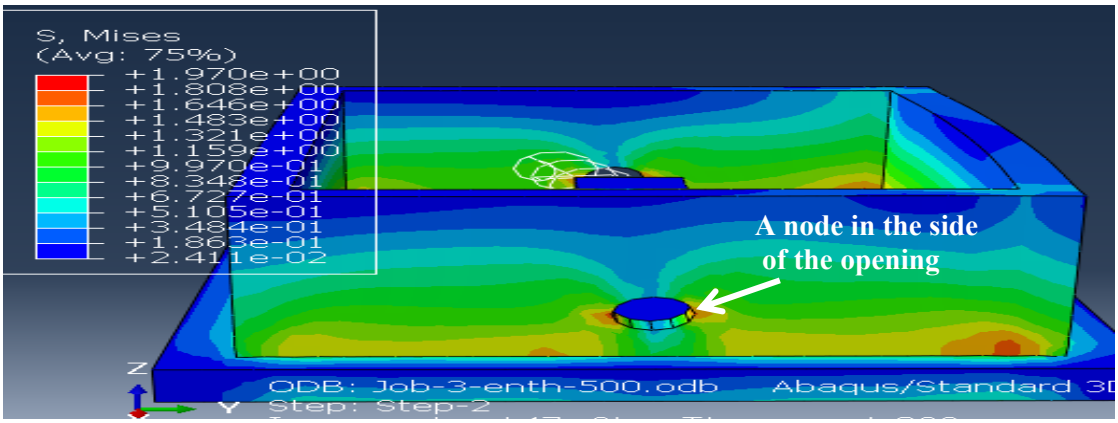


**(b) Tank with a hole in the wall**

**Figure (13): Von-Mises stress distribution**

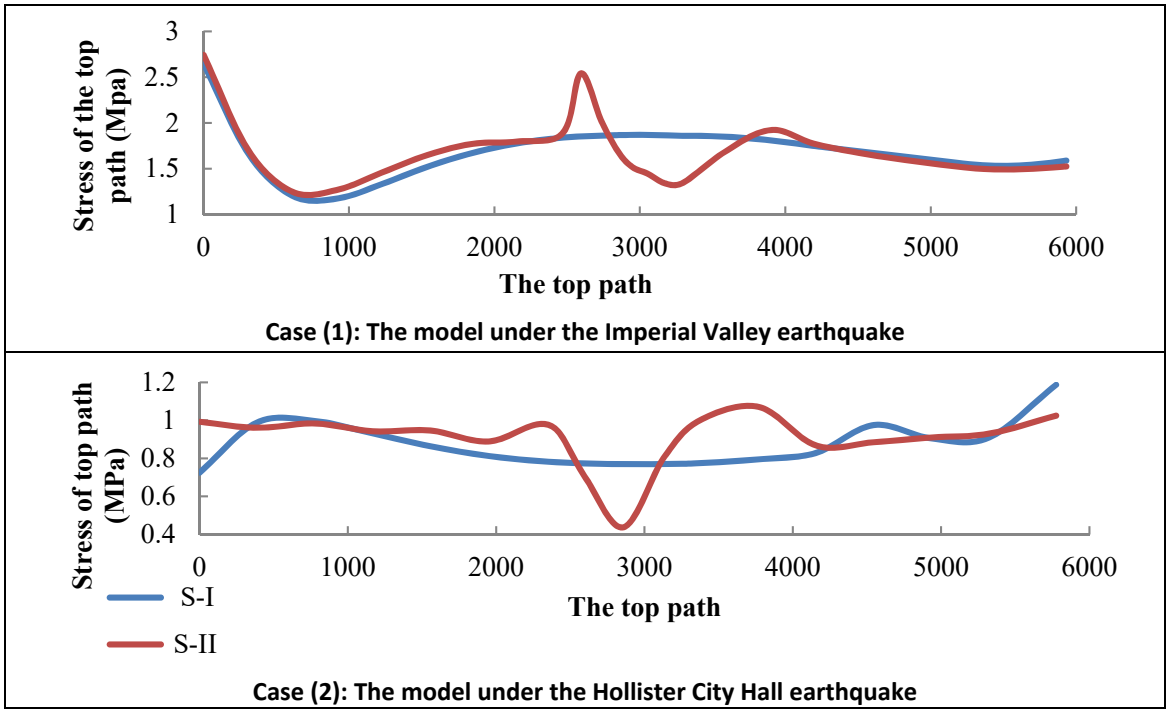


**Figure (14): Von-Mises stress of the top path of S-I and S-II models**

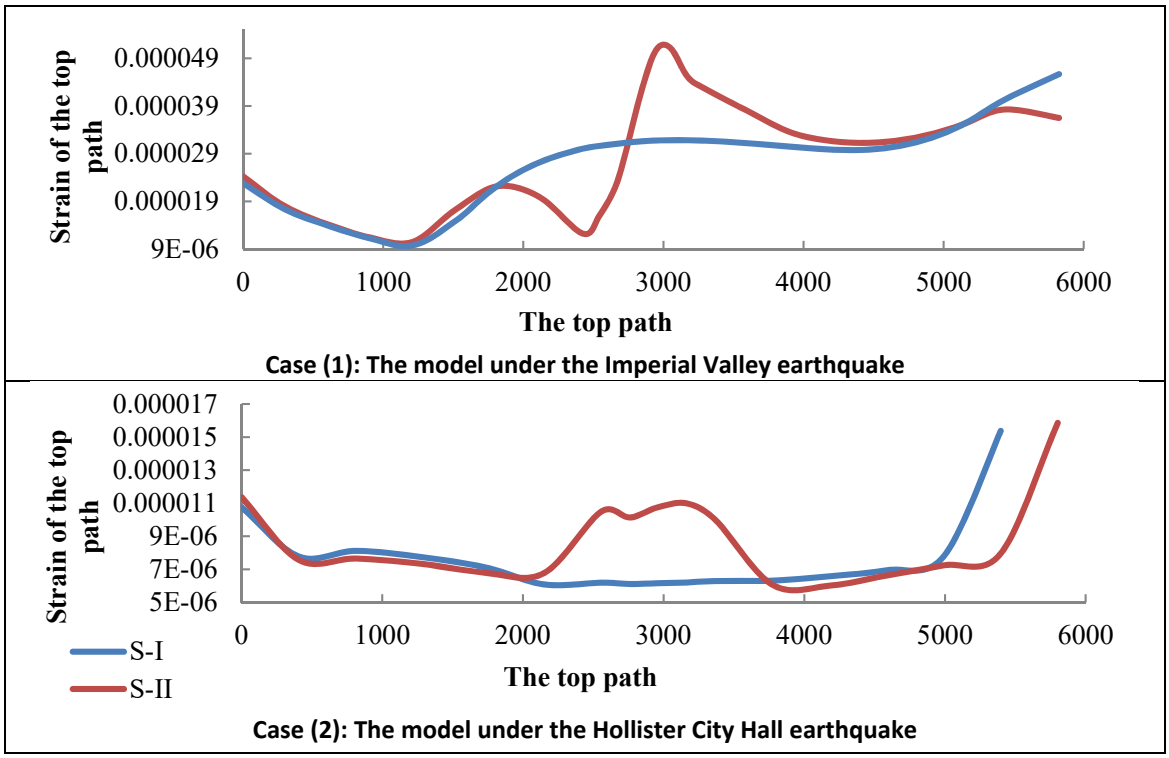


**Figure (15): Maximum principal strains of the top path of S-I and S-II**

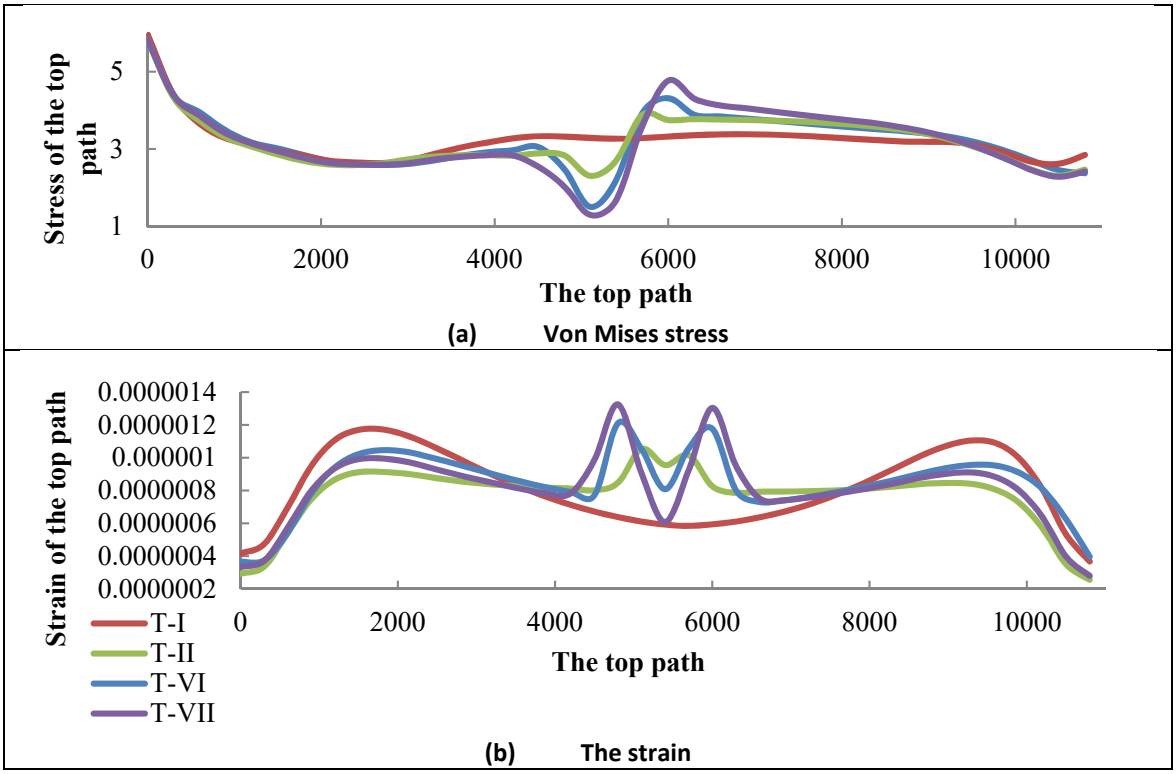


**Figure (16): Von-Mises stress and strain of the top path of T-I, T-II, T-VI and T-V-II models under the Imperial Valley earthquake**

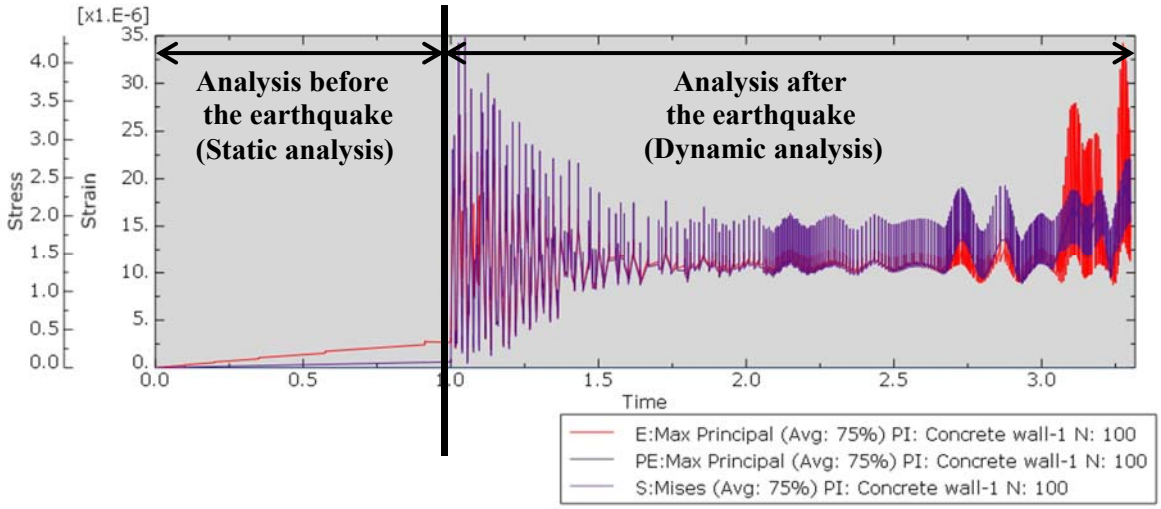


**Figure (17): Von-Misses stress and maximum principal strain on the opening adjacent side node for model S-II in static and dynamic analyses**

## CONCLUSIONS

The effect of openings embedded in reinforced concrete walls of the rectangular on-grade water tank under seismic force was investigated by nonlinear analysis finite element models in three- dimensional simulation using ABAQUS software. The hydrostatics, hydrodynamics and sloshing effect with an added-mass model were adopted in this numerical analysis. The rectangular tank was studied by analyzing eleven models with different parameters, which are the presence or absence of the holes in the walls, the position of the opening relative to the wall base, the direction of the opening compared to the direction of analysis, three earthquake accelerations and different openings diameters. The results of this research concluded the following:

- The presence of openings has a great effect on changing the distribution of stresses and strains in the tank walls. The stresses and strains were transferred from the center of the wall base to around the openings in the presence of a hole in the wall. Once the acceleration of an earthquake increases, the difference in stress and strain augments on both sides of the opening, making it more dangerous. Although the opening positions of the models T-II, T-VI and T-VII are located on one level and subjected to the same direction and magnitude of seismic forces, the values of stress and strain at the top of the openings for model T-VII are greater than for model T-VI and the values for the latter are greater than for model T-II. This increase in the values of stress and strain is a result of the difference in the diameter of the holes, as the greater the diameter, the greater the stress and strain.
- Despite the fact that S-II, S-III, T-II and T-III have identical opening diameters and position, the results of the analysis revealed that both the maximum equivalent stress around the opening and the maximum principal strain for S-II and T-II are greater than for the other models. This is attributed to the difference in the direction of the seismic loading compared with the opening position direction. Hence, this proved that the response of reinforced concrete on-grade water tank with embedded holes is sensitive to the direction of the earthquake loading.
- S-II, S-IV, T-II, T-IV and T-V have identical opening diameters and identical ground motion magnitude and direction relative to the opening position and direction. The result of this analysis showed that the maximum stress rises around the opening when the distance between the opening and the base decreases.

Last, but not least, water tank structure designers must take into account the direction of the seismic loading reference to the direction of the opening in the wall and its diameter, as well as the opening position analogous to the base.

## REFERENCES


ACI 350.3-06. (2006). "Seismic design of liquid-containing concrete structures." (ACI 350.3-06) and commentary (ACI 350.3R-06). American Concrete Institute, Farmington Hills, MI, U.S.A.

Al-Far, A., and Al-Far, S. (2016). "Seismic retrofitting study on an industrial building in Aqaba-Jordan." Jordan Journal of Civil Engineering, 10 (4).

Chen, J., and Kianoush, M. (2009). "Generalized SDOF system for seismic analysis of concrete rectangular liquid storage tanks." Engineering Structures, 31 (10), 2426-2435.

Code, S.B. (1994). "Southern building code congress international." Birmingham, AL, 35213.

Council, I. C. (2000). "International building code 2000." International Code Council.

Deoda, V., Adhikary, S., and Srinivasa Raju, V. (2020). "Seismic analysis of earthen dams subjected to spectrum compatible and conditional mean spectrum time histories." Jordan Journal of Civil Engineering, 14 (1).

EC8. (2000). "Design provisions for earthquake resistance of structures." Lausanne, Switzerland.

Ghateh, R., Kianoush, M., and Pogorzelski, W. (2015). "Seismic response factors of reinforced concrete pedestal in elevated water tanks." Engineering Structures, 87, 32-46.

Haroun, M.A. (1980). "Dynamic analyses of liquid storage tanks." California Institute of Technology.

Haroun, M.A., and Housner, G.W. (1981). "Seismic design of liquid storage tanks." Journal of the Technical Councils of ASCE, 107 (1), 191-207.

Hatayama, K. (2015). "Damage to oil storage tanks from the 2011 Mw 9.0 Tohoku-Oki Tsunami." Earthquake Spectra, 31 (2), 1103-1124.

Hazirbaba, K., Mughieda, O., and Abu-Lebdeh, G. (2019). "A critical review on seismic design of earth-retaining structures." Jordan Journal of Civil Engineering, 13 (1).

Housner, G. W. (1963). "The dynamic behavior of water tanks." Bulletin of the Seismological Society of America, 53(2), 381-387.

IITK, and GSDMA. (2005). "Guidelines for seismic design of liquid storage tanks." Provisions with Commentary on the Indian Seismic Code: Indian Standard IS 1893 (Part 1): 2002. Indian Institute of Technology Kanpur, Gujarat State Disaster Management Authority.

IS-3370. (1967). "Code of practice for concrete strutures for the storage of liquids." Bureau of Indian Standards, (Part IV)-1967.

Kumar, P.D., Aishwarya, A., and Maiti, P. (2016). "Comparative study of dynamic analysis of rectangular liquid filled containers using codal provisions." Procedia Engineering, 144, 1180-1186.

Malhotra, P.K. (1997). "New method for seismic isolation of liquid-storage tanks." Earthquake Engineering and Structural Dynamics, 26 (8), 839-847.

Manaul, A.A.U.S. (2014). "ABAQUS documentation version 6.14-1." Dassault Systems SIMULA Corp., Providence, RI, USA.

Munshi, J. A. (1998). "Rectangular concrete tanks." Portland Cement Association.

Munshi, J. A. (2002). "Design of liquid-containing concrete structures for earthquake forces." Portland Cement Association.

Officials, I.C.O.B. (1994). "Uniform building code." Structural Engineering Design Provisions.

Parish, S. (1999). "BOCA national building code compliance manual: 1996 BOCA national building code." McGraw-Hill Companies.

Rai, D.C. (2002). "Seismic retrofitting of R/C shaft support of elevated tanks." Earthquake Spectra, 18 (4), 745-760.

Seismosoft. (2002). "Earthquake engineering software solutions." https://seismosoft.com/products/seismospect/

Tedesco, J.W. (1983). "Vibrational characteristics and seismic analysis of cylindrical liquid storage tanks."

Uniform Building Code. (1997). "International conference of building officials." Uniform Building Code, Whittier, California.

Veletsos, A. (1974). "Seismic effects on flexible liquid storage tanks." Proceedings of the 5th World Conference on Earthquake Engineering.

Yazdanian, M., Ingham, J., Dizhur, D., and Kahanek, C. (2019). "A conspectus of wine storage tank damage data following the 2013 and 2016 New Zealand earthquakes." 2019 Pacific Conference on Earthquake Engineering.